*M&C 2017 - International Conference on Mathematics & Computational Methods Applied to Nuclear Science & Engineering, Jeju, Korea, April 16-20, 2017, on USB (2017)*

# TORT-TD Transient Simulations of the C5G7-TD Benchmark

A. Seubert, K. Velkov

*Gesellschaft für Anlagen- und Reaktorsicherheit (GRS) gGmbH, Forschungszentrum, Boltzmannstr. 14, D-85748 Garching, Germany*

**Abstract** - *This paper presents transient solutions of the C5G7-TD benchmark obtained with the time-dependent discrete-ordinates transport code TORT-TD. The applied code TORT-TD is summarized first, followed by a short description of the spatial discretization used to solve the 2-D and 3-D benchmark exercises. The presented TORT-TD solutions focus on dependencies on the spatial discretization in radial and axial direction as well as on impacts of the diffusion approximation and of the delayed neutron fraction on the power evolutions. The results of selected 2-D and 3-D transients are shown and discussed.*

## I. INTRODUCTION

The C5G7-TD benchmark [1] has been issued by the OECD/NEA Expert Group on Radiation Transport and Shielding (EGRTS) of the Working Party on Scientific Issues of Reactor Systems (WPRS) as a more transient follow-up of the past 3-D extension of the C5G7MOX fuel assembly steady state benchmark [2]. Being a pure computational problem, this benchmark extents the original idea of the preceding C5G7-2D and C5G7-3D benchmarks towards testing the ability of modern deterministic transport methods and codes to treat transient LWR core problems without spatial homogenization and without thermal-hydraulic feedback. GRS has participated in the C5G7-2D and 3D benchmarks [3, 4] using the discrete codes DORT and TORT.

In this paper, transient solutions for 2-D and 3-D problems of the C5G7-TD benchmark are presented which have been obtained with the time-dependent discrete-ordinates transport code TORT-TD [5]. As the benchmark specification is still under discussion and therefore subject to changes, the results may be regarded preliminary and also show solutions to problems which have been replaced by modified ones. In the following, the applied code TORT-TD is shortly described first, before the spatial discretizations used to solve the 2-D and 3-D benchmark exercises are explained. The presented TORT-TD solutions focus on dependencies on the spatial discretization in radial (circular pin modeling) and axial direction (number of meshes in the active core region) and on the impacts of the diffusion approximation and of the delayed neutron fraction on the power evolutions.

## II. THE TIME-DEPENDENT DISCRETE-ORDINATES TRANSPORT CODE TORT-TD

TORT-TD [5] is a time-dependent 3-D multi-group discrete ordinates ($S_N$) neutron transport code developed at GRS. It extends the DOORS steady-state neutron transport code TORT [6, 7] by a direct solution of the time-dependent few-group transport equation in 3-D with an arbitrary number of prompt and delayed neutron precursor groups in both Cartesian and cylindrical 3-D geometry. Unconditional numerical stability in transient calculations is achieved using a fully implicit time discretization scheme. Scattering anisotropy is treated in terms of a $P_l$ Legendre scattering cross-section expansion. The macroscopic cross sections can be supplied in terms of tabulated cross section libraries, which allow functionalizations with respect to thermal-hydraulic feedback parameters. In TORT-TD transient operation mode, computing time can be saved by extrapolating the angular neutron fluxes to the next time step using the space-energy resolved inverse reactor period.

TORT-TD major fields of application include Light Water Reactors (LWR) with geometric description at pin cell and sub pin cell level, source-driven sub-critical systems (e.g. ADS) and high-temperature gas cooled reactors (V/HTR) [8]. Thermal-hydraulic feedback is accounted for by couplings with ATHLET [5], COBRA-TF [9] and ATTICA3D [10]. For LWR applications, Generalized Equivalence Theory (GET) at pin cell level has been implemented in TORT-TD in terms of pin cell discontinuity factors in order to reduce pin cell homogenization errors [11]. For the simulation of subcritical systems, TORT-TD has been extended to account for external time-dependent distributed neutron sources [12]. A similar approach has been recently implemented into the PARCS code with the aim to simulate fast spectrum source-driven systems (see a separate paper at this conference [13]). For fast running scoping calculations, a fine-mesh 3-D diffusion solver is also implemented in TORT-TD, which operates on the same space-energy discretization, and so can be used to quantify deviations coming from the diffusion approximation. Movement of control rods is implemented by applying a flux-volume weighting approach for the cross sections at the control rod tips, when the control rod tip is in between adjacent axial mesh boundaries.

## III. SPATIAL DISCRETIZATION OF THE PROBLEM DOMAIN

Similar to the preceding problems of the C5G7 benchmark series, no spatial homogenization should be applied

within the pin cell. This requires a suitable approximation of the circular shape of a single fuel rod when using Cartesian coordinates. The spatial discretization in radial direction is based on the approach applied with DORT and TORT in the past C5G7-2D [3] and C5G7-3D-Extension [4] benchmarks. As shown in Fig. 1, the circular pin boundary is approximated by a stair case function such that the cross sectional area is preserved. This results in additional meshes within the pin cell, e.g. 7x7=49 in the example of Fig. 1; the simplest approximation is given by a square representation of the pin. While the stair case model ensures preservation of the pin area, the pin circumference keeps constant, i.e. is independent of the number of steps, although the approximation of the circular boundary appears to improve.

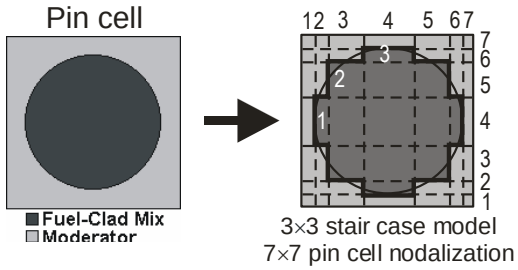


Fig. 1: Discretization of the pin cell on the Cartesian grid.

Fig. 2 shows the C5G7 discretization in radial direction using a 2x2 stair case pin approximation. This results in a total of 221x221=48841 spatial nodes in the radial plane. In axial direction, the fissile height (active core) has been discretized in either 36 or 24 equidistant meshes with corresponding mesh sizes of 3.57 cm and 5.355 cm, respectively. For the upper and lower axial reflectors, a mesh size of 7.14 cm has been used, amounting to 3 meshes per reflector. This results in a total of 0.98 million spatial meshes for the 1x1 stair case pin discretization in combination with 42 axial meshes and 1.46 million spatial meshes for the 2x2 stair case pin discretization in combination with 30 axial meshes. This requires around 3 GB of memory which, however, also includes additional large arrays to store the adjoint neutron flux distribution for dynamic reactivity evaluations and a couple of large arrays for post processing of spatial distributions of neutron flux, power density and up to six thermal hydraulics parameters. The calculation time, measured on a standard PC with a Core-i7 processor, ranges between a few hours for the diffusion approximation and a few days for the transport simulation (TORT-TD is a serial code, i.e. not parallelized).

In the following, results of selected 2-D and 3-D transients are shown. All transients have been simulated with a constant time step size of 0.05 s; this amounts to a number of 320 time steps for a problem time of 16 s (3-D transients). The simulations are based on the provided macroscopic cross section data in 7 energy groups and the given delayed neutron data in 8 precursor time groups. The transport calculations have been carried out using $S_4$ level-symmetric quadrature. For comparison, diffusion approximation solutions have also been obtained with the same spatial meshing and nuclear group data.

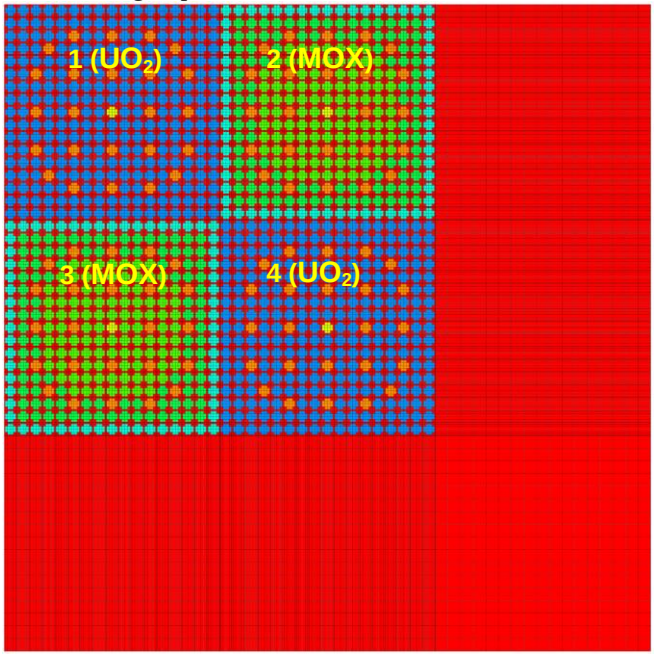


Fig. 2: Radial view of the discretized C5G7 problem geometry within fissile zone. The colors denote different materials and corresponding cross section sets.

## IV. RESULTS FOR 2-D PROBLEMS TD1 AND TD2

The TD1 and TD2 problems are 2-D problems and simulate control rod insertion (equal to 1 % and 10 %, respectively, of the active core height) and withdrawal transients by linear temporal changes of the guide tube cross sections. TD1-1 and TD2-1 simulate insertion and withdrawal of bank 1 (see Fig. 2), TD1-2/TD2-2 and TD1-3/TD2-3 insertion and withdrawal of bank 3 and 4, respectively. In all these cases, the control rod insertions occur within the first second after the beginning of the transient; the withdrawals are simulated within the next second. Results for the power evolutions of the first three 2-D exercises TD1 are shown in Fig. 3. Therein, the transport solutions (shown with solid lines) are compared to corresponding diffusion calculations (shown with dashed lines). It can be seen that the diffusion solutions slightly differ from the corresponding transport calculations. Corresponding $S_4$ transport calculation results for the TD2 cases are given in Fig. 4. Normalized distributions of thermal neutron flux and power density at the beginning of the transients are depicted in Fig. 5 and Fig. 6, respectively.

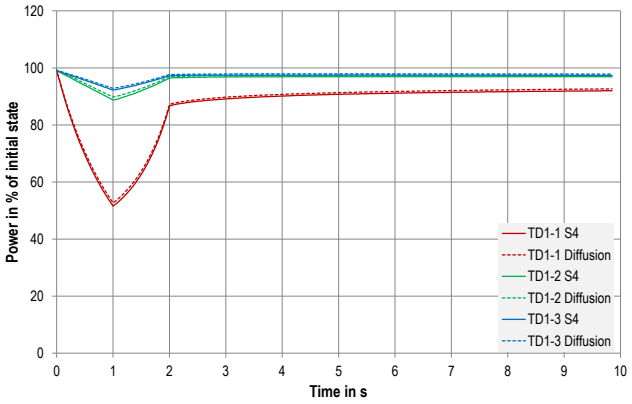


Fig. 3: TORT-TD normalized power evolutions for the first three 2-D exercises TD1. Solid and dashed lines denote transport and diffusion calculations.

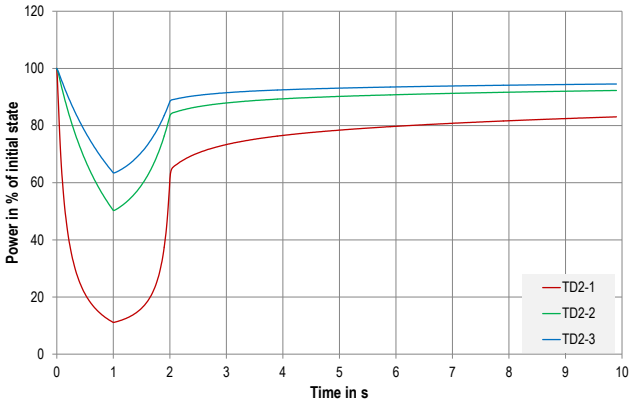


Fig. 4: TORT-TD normalized power evolutions for the three 2-D exercises TD2 obtained with $S_4$ transport solution.

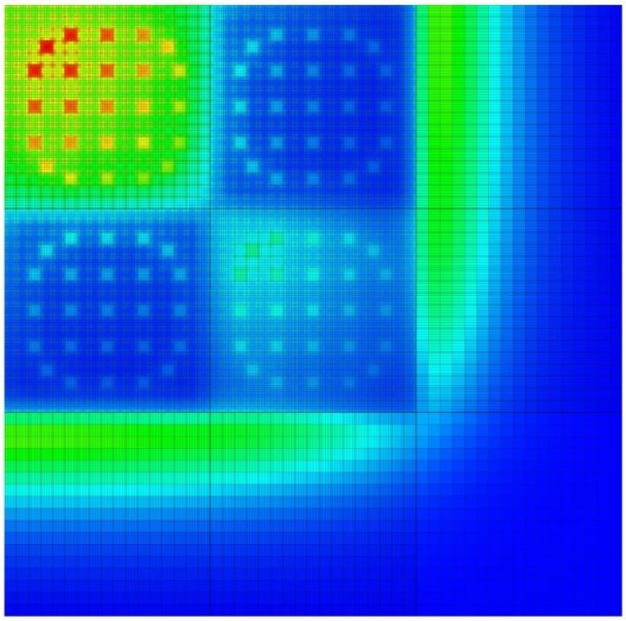

Fig. 5: Thermal flux distribution at the beginning of the transients TD1 and TD2.

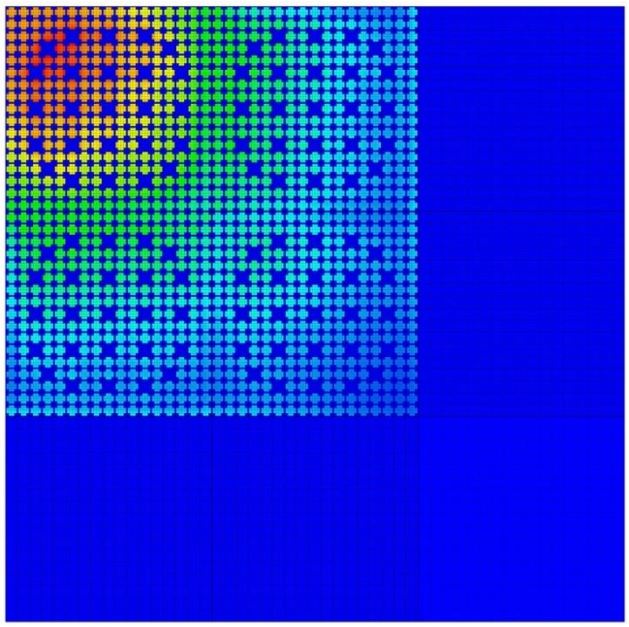

Fig. 6: Power density distribution at the beginning of the transients TD1 and TD2.

## V. RESULTS FOR THE 3-D PROBLEMS TD4

The TD4 transients are 3-D problems in which control rod withdrawal and insertion events for single control rod banks or combinations of different control rod banks are simulated:

- TD4-1: bank 1 insertion and withdrawal
- TD4-2: bank 3 insertion and withdrawal
- TD4-3: bank 1 and 3 insertion and withdrawal
- TD4-4: bank 3 and 4 insertion and withdrawal
- TD4-5: bank 1 and 3 insertion and withdrawal

In the following, results for the five 3-D transient cases TD4 are shown. Because of a change of the TD4-4 definition in the benchmark specification v1.6, both TD4-4 simulations have been done. They have been obtained for 24 axial meshes within the fissile height and a 2x2 stair case model of the pin (denoted by n2z24).

### 1. Comparison between S4 Transport and Diffusion Approximation

To study the impact of the diffusion approximation, each transient has been simulated with both $S_4$ transport theory and diffusion approximation, while any other parameter, e.g. the spatial meshing, is unchanged. Obviously, there are only slight differences between transport and diffusion solutions; the diffusion approximation tends to underestimate the overall power evolutions. Regarding the

case TD4-4, Fig. 10 shows results according to the original definition of this transient, whereas Fig. 12 refers to the new definition used in benchmark specification v1.6.

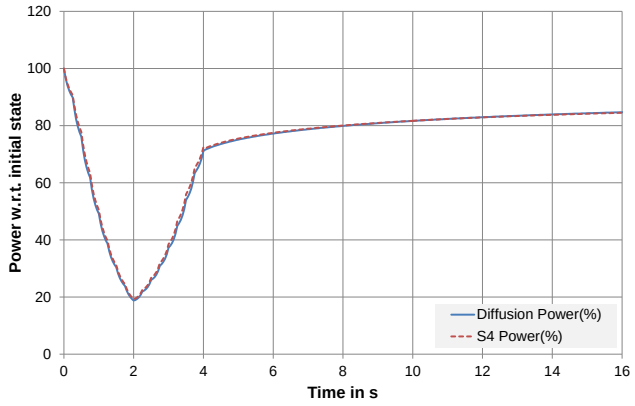


Fig. 7: Power evolution of the TD4-1 transient obtained with S4 transport theory (dashed line) and diffusion approximation (solid line) for 2x2 pin model and 24 axial meshes.

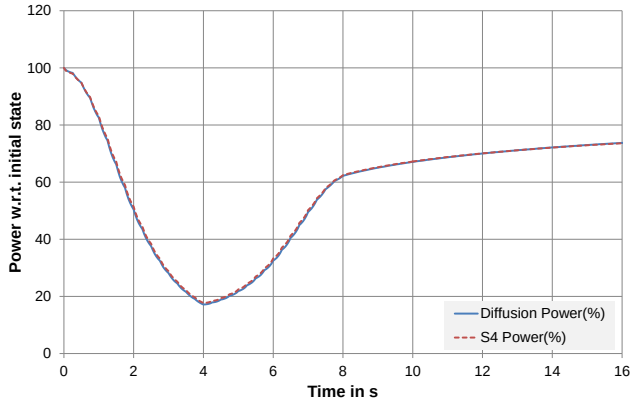


Fig. 8: Power evolution of the TD4-2 transient obtained with S4 transport theory (dashed line) and diffusion approximation (solid line) for 2x2 pin model and 24 axial meshes.

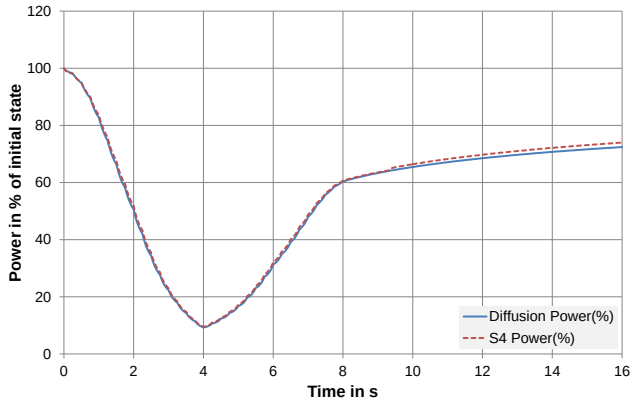


Fig. 9: Power evolution of the TD4-3 transient obtained with S4 transport theory (dashed line) and diffusion approximation (solid line) for 2x2 pin model and 24 axial meshes.

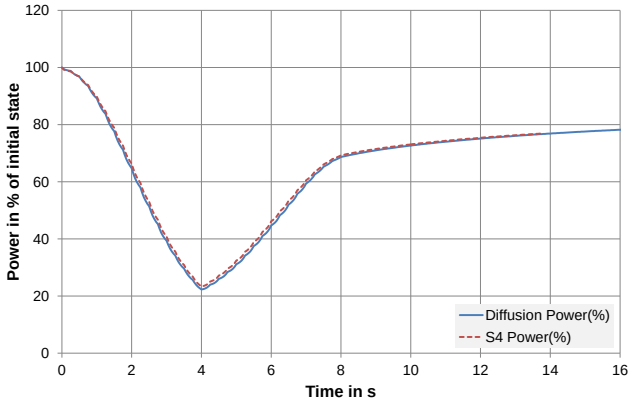


Fig. 10: Power evolution of the TD4-4 transient obtained with S4 transport theory (dashed line) and diffusion approximation (solid line) for 2x2 pin model and 24 axial meshes.

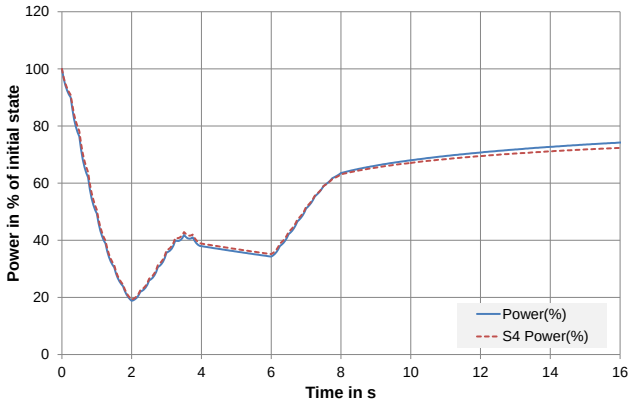


Fig. 11: Power evolution of the TD4-5 transient obtained with S4 transport theory (dashed line) and diffusion approximation (solid line) for 2x2 pin model and 24 axial meshes.

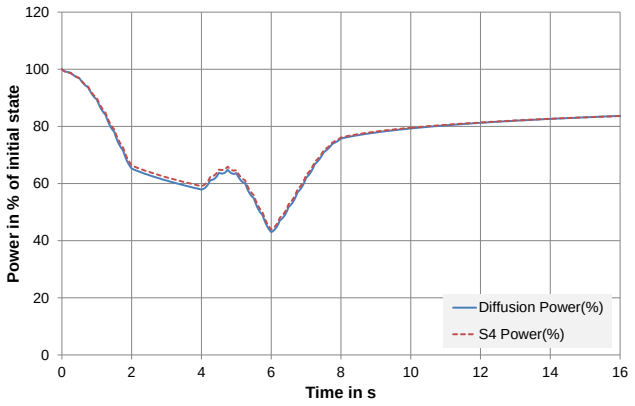


Fig. 12: Power evolution of the TD4-4 (v1.6) transient obtained with S4 transport theory (dashed line) and diffusion approximation (solid line) for 1x1 pin model and 24 axial meshes.

## 2. Comparison between Different Spatial Discretizations

Although the control rod cusping effect remains relatively small, it becomes visible in, e.g., the case TD4-5 between $t = 3$ s and $t = 4$ s. During this period, the control rods of bank 1 are being withdrawn again, while the control rods of bank 3 are being inserted. Given a control rod movement speed of 21.42 cm/s, the control rod moves by 1.071 cm during a single time step of 0.05 s. This means that for a mesh size of 5.355 cm corresponding to 24 meshes within the axial fissile height, the control rod tip stays within one axial mesh for 5 time steps. For a mesh size of 3.57 cm (36 axial meshes), the control rod tip moves from one axial mesh to the next every 3.33 time steps. This results in a reduced control rod cusping effect, as shown in Fig. 13.

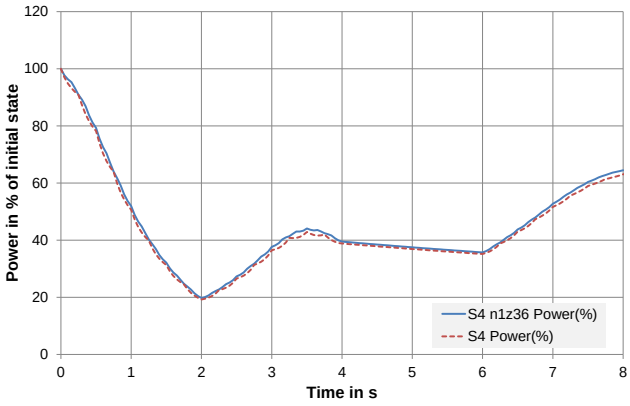


Fig. 13: Comparison of $S_4$ transport solutions for case TD4-5 between 36 (solid line, 1x1 pin model) and 24 (dashed line, 2x2 pin model) axial meshes.

## 3. Influence of the Effective Delayed Neutron Fraction

In order to study the influence of the delayed neutrons on the power evolutions of the 3-D transient cases TD4, the effective delayed neutron fraction has been varied. For having two enveloping cases for each of the TD4 transient, each TD4 transient has been simulated with either the highest delayed neutron fraction, given by $\beta = 701$ pcm for $UO_2$ fuel, and the lowest delayed neutron fraction, given by $\beta = 335$ pcm for MOX fuel. In each case, $\beta$ is applied as a global value for the whole core. The calculations have been carried out for 24 axial meshes within the fissile height, a 1x1 stair case model of the pin and diffusion approximation. The results obtained for the five TD4 transients are depicted in Fig. 14 through Fig. 18, where for the TD4-4 case the modified definition given in specification revision 1.6 has been utilized. As expected, application of the delayed neutron fraction of $UO_2$ results in more gentle evolutions, whereas the corresponding MOX value provides the opposite behavior.

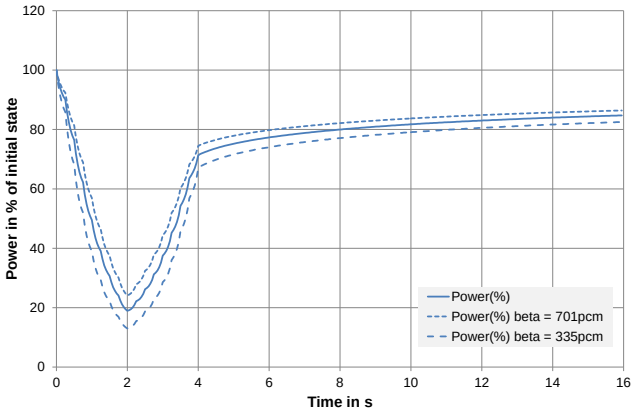


Fig. 14: Power evolutions of the TD4-1 transient obtained for $\beta_{UO2}$ (dotted line) and $\beta_{MOX}$ (dashed line).

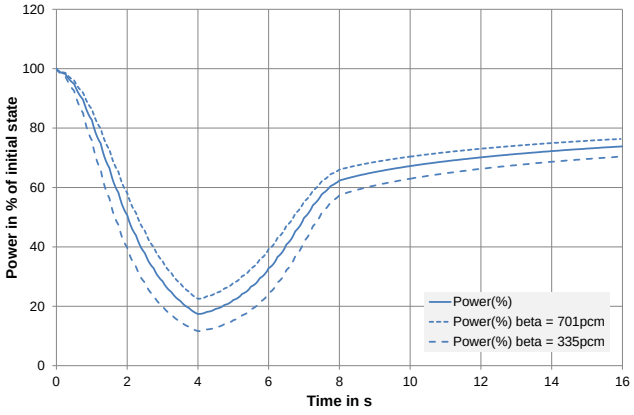


Fig. 15: Power evolutions of the TD4-2 transient obtained for $\beta_{UO2}$ (dotted line) and $\beta_{MOX}$ (dashed line).

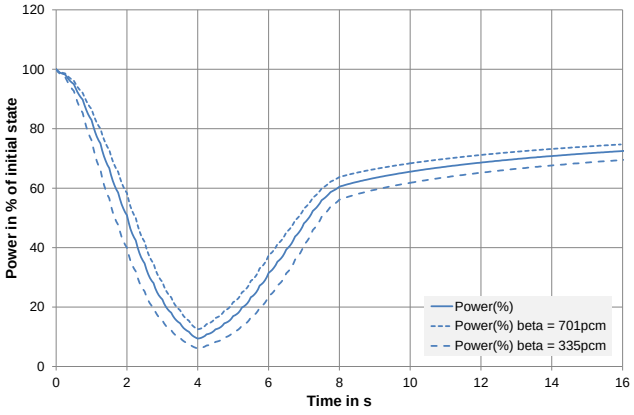


Fig. 16: Power evolutions of the TD4-3 transient obtained for $\beta_{UO2}$ (dotted line) and $\beta_{MOX}$ (dashed line).

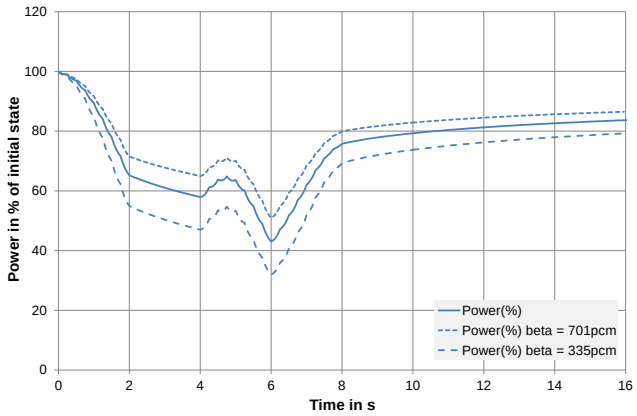


Fig. 17: Power evolutions of the TD4-4 (v1.6) transient obtained for $\beta_{UO2}$ (dotted line) and $\beta_{MOX}$ (dashed line).

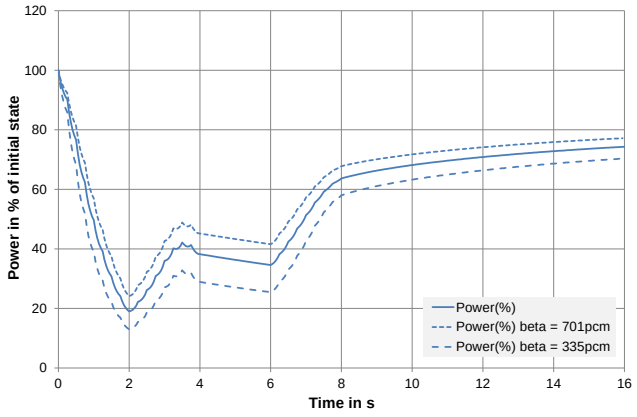


Fig. 18: Power evolutions of the TD4-5 transient obtained for $\beta_{UO2}$ (dotted line) and $\beta_{MOX}$ (dashed line).

## VI. SUMMARY

This paper shows 2-D and 3-D transient solutions of the C5G7-TD benchmark which were obtained by the time-dependent discrete-ordinates transport code TORT-TD. The heterogeneity at pin cell level is modeled in Cartesian co-ordinates by approximating the circular shape of the pin by a staircase boundary such that the pin's circular cross sectional area is preserved. The transport results shown in terms of total power evolutions are supplemented by corresponding calculations using the diffusion approximation on the same spatial meshing, so giving an idea of the quality of the solution methods.

## REFERENCES

1. V. F. Boyarinov et al., "Deterministic Time-Dependent Neutron Transport Benchmark without Spatial Homogenization (C5G7-TD)", NEA/NSC/DOC(2016), OECD Nuclear Energy Agency, July 2016.
2. M. A. Smith, G. Palmiotti, T. A. Taiwo, E. E. Lewis, N. Tsoulfanidis, Benchmark Specification for Deterministic MOX Fuel Assembly Transport Calculations without Spatial Homogenisation (3-D Extension C5G7 MOX). NEA/NSC/DOC(2003) 6.
3. S. Langenbuch, A. Seubert, W. Zwermann, "Results on the DECD/NEA C5G7-MOX benchmark obtained with the discrete ordinates code DORT", Prog. Nucl. Energy **45** (2004) 153-168.
4. A. Seubert, W. Zwermann, S. Langenbuch, "Solution of the C5G7 3-D extension benchmark by the SN code TORT", Prog. Nucl. Energy **48** (2006) 432-438.
5. Seubert, K. Velkov, S. Langenbuch, "The Time-Dependent 3-D Discrete Ordinates Code TORT-TD with Thermal-Hydraulic Feedback by ATHLET Models", Proc. PHYSOR 2008, Interlaken, Switzerland, September 14–19, 2008, American Nuclear Society (2008) (CD-ROM).
6. W. A. Rhoades, R. L. Childs, "The TORT three dimensional discrete ordinates neutron/photon transport code", Nucl. Sci. Eng., 107, 397 (1991).
7. W. A. Rhoades, D. B. Simpson, "The TORT Three dimensional Discrete Ordinates Neutron/Photon Transport Code (TORT Version 3)", ORNL/TM-13221.
8. A. Seubert, "The Time-Dependent 3-D Transport Code TORT-TD: Recent Advances and Applications", Transactions of the American Nuclear Society, Vol. 104, Hollywood, Florida, June 26–30, 2011.
9. M. Christienne, M. Avramova, Y. Perin, A. Seubert, "Coupled TORT-TD/COBRA-TF Capability for High-Fidelity LWR Core Calculations", Proc. PHYSOR 2010, Pittsburgh, USA, May 9–14, 2010, American Nuclear Society (2010) (CD-ROM).
10. Seubert, A. Sureda, J. Lapins, J. Bader, E. Laurien, "The Transient 3-D Transport Coupled Code TORT-TD/ATTICA3D for High-Fidelity Pebble-Bed HTGR Anal-yses", Transp. Theory and Stat. Phys., 41, 133, 2012.
11. Seubert, "Pin Cell Discontinuity Factors in the Transient 3-D Discrete Ordinates Code TORT-TD", Proc. PHYSOR 2010, Pittsburgh, USA, May 9–14, 2010, American Nuclear Society (2010) (CD-ROM).
12. Seubert, A. Pautz, M. Becker, R. Dagan, "Time-dependent Anisotropic distributed Source Capability in Transient 3-D Discrete Ordinates Code TORT-TD", Inter-national Conference on Mathematics, Computational Methods & Reactor Physics (M&C 2009), Saratoga Springs, USA, May 3–7, 2009.
13. A. Mantout, A. Seubert, K. Velkov, „Time-Dependent External Distributed Neutron Source Capability in PARCS and Comparison with TORT-TD", M&C 2017 - International Conference on Mathematics & Computa-

tional Methods Applied to Nuclear Science & Engineering, Jeju, Korea, April 16-20, 2017, on USB (2017).